

Search for the differences in Atmospheric Neutrinos and Antineutrinos oscillation parameters at the INO-ICAL Experiment

Daljeet Kaur*, Zubair Ahmad Dar[‡], Sanjeev Kumar[†], Md. Naimuddin[†]

*S.G.T.B. Khalsa college, University of Delhi

[‡]Aligarh Muslim University, Aligarh

[†]Department of Physics and Astrophysics, University of Delhi

10 March 2017

Abstract

In this paper, we present a study to measure the differences between the atmospheric neutrino and anti-neutrino oscillations in the Iron-Calorimeter detector at the India-based Neutrino Observatory experiment. Charged Current ν_μ and $\bar{\nu}_\mu$ interactions with the detector under the influence of earth matter effect have been simulated for ten years of exposure. The observed ν_μ and $\bar{\nu}_\mu$ events spectrum are separately binned into direction and energy bins, and a χ^2 is minimised with respect to each bin to extract the oscillation parameters for ν_μ and $\bar{\nu}_\mu$ separately. We then present the ICAL sensitivity to confirm a non-zero value of the difference in atmospheric mass squared of neutrino and anti-neutrino i.e. $|\Delta m_{32}^2| - |\Delta \bar{m}_{32}^2|$.

1 Introduction

In the last few decades, neutrino oscillation experiments have provided many model independent evidences of neutrino oscillations. It all started in 1998 when Super-Kaimokande observed that the atmospheric muon neutrinos are changing flavor as they traverse through the atmosphere [1, 2]. In 2001, the Sudbury Neutrino Observatory experiment obtained a direct evidence of a flavor change of solar neutrinos due to neutrino oscillations [3]. Next, KamLand experiment observed the same effect with reactor neutrinos in 2002 [4]. There are now multiple next generation of experiments aimed at studying neutrino oscillation using different neutrino sources. The neutrino oscillations within the three flavor framework is well established from solar, atmospheric and reactor neutrino experiments, and the oscillation parameters are getting measured with better precision. The evidence of non-zero masses of neutrinos establish the fact that the three flavors of neutrinos are mixed. In the three-flavor oscillation paradigm, neutrino mixing can be described by a 3×3 unitary mixing matrix known as Pontecorvo-Maki-Nakagawa-Sakata (PMNS) matrix [5, 6]. The three flavor eigenstates of neutrinos are mixtures of three mass eigenstates according to the PMNS matrix. Under the standard parameterization of PMNS matrix, the neutrino oscillation probabilities are defined in terms of three mixing angles θ_{12} , θ_{23} , θ_{13} ; two mass-squared differences Δm_{21}^2 , Δm_{32}^2 and a Dirac CP-violation phase δ_{CP} . The resulting oscillation probabilities depends on the these oscillation parameters (mixing angles and mass squared differences). For a given neutrino of energy E_ν and the propagation length L , the survival probability for ν_μ is given by

$$P(\nu_\mu \rightarrow \nu_\mu) \simeq 1 - 4 \cos^2 \theta_{13} \sin^2 \theta_{23} \times [1 - \cos^2 \theta_{13} \sin^2 \theta_{23}] \sin^2\left(\frac{1.267 |\Delta m_{32}^2| L}{E_\nu}\right), \quad (1)$$

and similarly the survival probability for $\bar{\nu}_\mu$ is given by

$$P(\bar{\nu}_\mu \rightarrow \bar{\nu}_\mu) \simeq 1 - 4 \cos^2 \bar{\theta}_{13} \sin^2 \bar{\theta}_{23} \times [1 - \cos^2 \bar{\theta}_{13} \sin^2 \bar{\theta}_{23}] \sin^2\left(\frac{1.267 |\overline{\Delta m_{32}^2}| L}{E_{\bar{\nu}}}\right), \quad (2)$$

where, the symbols with bar ($|\overline{\Delta m_{32}^2}|, \bar{\theta}_{13}, \bar{\theta}_{23}$) are used for the respective parameters for the anti-neutrino oscillations.

In the Standard Model (SM) of particle physics, the parameters for particles and antiparticles are identical because of CPT symmetry. Hence, under the CPT symmetry, the mass splittings and mixing angles are identical for neutrinos and anti-neutrinos, implying $P(\nu_\mu \rightarrow \nu_\mu) = P(\bar{\nu}_\mu \rightarrow \bar{\nu}_\mu)$. Any inequality between these disappearance probabilities of neutrinos and antineutrinos, could therefore, provide a hint for new physics. Also, any difference between the parameters governing the oscillation probabilities of neutrinos and

antineutrinos could provide a possible hint for CPT violation. We investigate the prospects for the measurement of such a difference in $|\Delta m_{32}^2|$ and $|\overline{\Delta m}_{32}^2|$ in Iron-Calorimeter (ICAL) experiment at the India-based Neutrino Observatory (INO) [7, 8]. A similar work has been carried out by MINOS [9] and Super-Kamiokande [10] experiment. However, in the present work, for the first time, we show the INO-ICAL experimental sensitivity for the difference in $|\Delta m_{32}^2|$ and $|\overline{\Delta m}_{32}^2|$ irrespective of the theoretical mechanism responsible for the difference in the neutrino and antineutrino parameters.

The INO-ICAL experiment is an atmospheric neutrino experiment meant to study neutrino oscillations with muon disappearance channel. The ICAL experiment is sensitive to the atmospheric muon type neutrinos and antineutrinos through their interactions with the iron target producing muons and hadrons via the Charged Current (CC) interactions. The ν_μ and $\bar{\nu}_\mu$ particles are identified by the production of μ^- and μ^+ , respectively, through their CC interaction ($\nu_\mu(\bar{\nu}_\mu) + X \rightarrow \mu^-(\mu^+) + X'$). The energy and direction of the incoming neutrinos/anti-neutrinos has to be measured accurately for the precise measurement of oscillation parameters. The energy and direction of these interacting neutrinos/anti-neutrinos can be determined from the reconstructed energy and direction of muons and hadrons. The muons deposit their energy in iron target forming a clear track-like pattern while hadrons form a shower-like pattern. Further details of the INO-ICAL experiment are provided in Sec. 2.

In this paper, we present the separate measurement of neutrino and anti-neutrino oscillation parameters. The INO-ICAL detector has a unique ability to distinguish between μ^- and μ^+ events with their bendings in magnetic field, and hence can easily separate neutrinos and anti-neutrinos. Earlier ICAL analysis has shown its potential for measurement of oscillation parameters and mass hierarchy with combined neutrino and anti-neutrino events [11, 12, 13, 14]. The reach of INO-ICAL experiment for CPT violation has also been studied in the literature [15, 16]. Here, we will analyze neutrino and anti-neutrino events separately and compare their oscillation parameters in order to find any signature of new physics including CPT violation [17, 18].

The analysis is performed with the construction of a χ^2 function with 3D binning in muon energy, muon direction and hadron energy [Sec. 3.1]. We calculate χ^2 for neutrinos and antineutrinos separately and minimize it to constraint the experimental parameter spaces ($|\Delta m_{32}^2|, \theta_{23}$) and ($|\overline{\Delta m}_{32}^2|, \bar{\theta}_{23}$) [Sec. 3.2] assuming that the true parameters of ν_μ and $\bar{\nu}_\mu$ are identical. Next, we study the possibility that the true values of $|\Delta m_{32}^2|$ and $|\overline{\Delta m}_{32}^2|$ can be different. In Sec. 3.3, we consider 4 theoretical scenarios when $|\Delta m_{32}^2|$ and $|\overline{\Delta m}_{32}^2|$ take different set of values to find the $\Delta\chi^2$ contours for different experimental values of $|\Delta m_{32}^2|$ and $|\overline{\Delta m}_{32}^2|$. This gives us the INO-ICAL sensitivity in the ($|\Delta m_{32}^2|$ - $|\overline{\Delta m}_{32}^2|$) parameter space for these hypothetical scenarios.

The main aim of the paper is to find the sensitivity of INO-ICAL for the measurement of the difference ($|\Delta m_{32}^2| - |\overline{\Delta m}_{32}^2|$). If the true values of the $|\Delta m_{32}^2|$ and $|\overline{\Delta m}_{32}^2|$ are different, at what confidence level the null hypothesis i.e. $|\Delta m_{32}^2| = |\overline{\Delta m}_{32}^2|$, can be ruled out? This is addressed in Sec. 3.4.

In this paper, we have demonstrated the potential of INO-ICAL for the separate measurement of ν_μ and $\bar{\nu}_\mu$ oscillation parameters. The results of this study are summarized in Sec. 4.

2 The ICAL experiment

India-based Neutrino Observatory (INO) is an approved mega science project, which will be located at Bodi West hills in the Theni district of South India. A huge 50 Kton ICAL detector with the magnetized iron target will operate at INO. The 1 km rock overburden above the site will act as a natural shield from the background of cosmic rays. The dimensions of the cavern will be $132m \times 26m \times 32m$. The ICAL detector will be of rectangular shape of dimensions $48m \times 16m \times 14.5m$ having three modules. Each module weighing about 17 Kton with the dimensions $16m \times 16m \times 14.5m$. Each module will consist of 151 layers of 5.6 cm thick iron plates with alternate gaps of 4 cm where the active detector element will be placed. The ICAL experiment will use Resistive Plate Chambers as active detector element to detect the charged particles produced in the neutrino interaction with the iron nuclei. Since the INO experiment is expected to take data for several years to collect statistically significant number of interactions, the RPCs are a good choice because of their long lifetime[19]. The RPCs will give (X, Y) hit information with 0.96 cm spatial resolution. There will be a total of 30,000 RPCs of dimension $2m \times 2m$ in the ICAL detector. Another important feature of the INO-ICAL experiment is the application of a magnetic field of 1.5 T that will help in distinguishing the charge of the interacting particles. This distinction is crucial for the precise determination of relative ordering of neutrino mass states (neutrino mass hierarchy) and other parameters.

The INO-ICAL experiment is sensitive to atmospheric muons only. Hence, it will observe interactions of muon type neutrinos. The detector is not suitable for detection of electrons because of large thickness of iron plates (5.6 cm) compared to the radiation length of iron (17.6 cm). Also, tau lepton production is limited because of the high threshold of tau production (4 GeV). The ICAL experiment will also measure the energy of hadron shower to improve the energy reconstruction of events, and hence the overall sensitivity to neutrino parameters[20, 13].

The INO-ICAL resolutions for muon energy and direction as well as hadron energy are available from the GEANT4 [21] simulation studies [22, 23]. The simulation studies provide us a reasonable characterization of the detector.

3 Analysis procedure

The magnetized ICAL detector is primarily designed to differentiate the neutrino and anti-neutrino interactions of atmospheric muon neutrinos with excellent charge identification [22]. Since the events at ICAL can easily be separated into samples of ν_μ and $\bar{\nu}_\mu$, they can be used to study oscillations separately in neutrinos and anti-neutrinos. We exploit this feature of ICAL experiment to measure the oscillation parameters independently using ν_μ and $\bar{\nu}_\mu$ events assuming $|\Delta m_{32}^2| = |\Delta \bar{m}_{32}^2|$. Next, we explore the ICAL ability to find out any non-zero difference in the atmospheric mass squared differences of neutrinos and antineutrinos i.e. $|\Delta m_{32}^2| - |\Delta \bar{m}_{32}^2|$.

For performing the analysis, we generated the atmospheric neutrino data set using HONDA et.al.[24] 3-D neutrino flux with ICAL detector specifications using NUANCE event generator [25]. For final χ^2 analysis, 1000 years equivalent data of 50kt ICAL detector has been scaled down to 10 years exposure to normalize the statistical fluctuations. The ICAL detector is highly sensitive for the CC interactions of ν_μ and $\bar{\nu}_\mu$ events in the energy range 0.8-12.8 GeV. Therefore, full event spectrum comprises the CC ν_μ (and $\bar{\nu}_\mu$) events coming from $\nu_\mu(\bar{\nu}_\mu) \rightarrow \nu_\mu(\bar{\nu}_\mu)$ survival channel and from $\nu_e(\bar{\nu}_e) \rightarrow \nu_\mu(\bar{\nu}_\mu)$ oscillation channel. Initially, each event is generated without introducing oscillations, to reduce the computational time. The effect of oscillations have been incorporated separately using the Monte Carlo re-weighting algorithm described in earlier studies [12, 14, 13]. For each neutrino/antineutrino event of a given energy (E_ν or $E_{\bar{\nu}}$) and zenith direction θ_z , three flavor oscillation probabilities are calculated taking earth matter effects into account. The matter density profile of Earth is taken from the Preliminary Reference Earth Model [26] which divides the Earth into several layers according to their matter densities.

In order to introduce the detector effects, we use the realistic detector resolutions and efficiencies of the ICAL detector based on GEANT4 simulations. The reconstruction of a neutrino (or anti-neutrino) event requires the measurement of the secondary particles like muons (or anti-muon) and hadrons. The muons give clear track of hits inside the magnetized detector. Therefore, the energy of these particles can be easily reconstructed using a track fitting algorithm. The complete details of ICAL response for μ^+ or μ^- e.g. energy and direction resolutions, reconstruction and charge identification efficiencies are available in Ref [22]. The ICAL has an excellent charge identification efficiency (more than 98%) and good direction resolution for muons ($\sim 1^\circ$) in the energy region of interest. Hadrons deposit their energies in a shower like pattern in the detector. So, total energy deposited by the hadron shower ($E'_{had} = E_\nu - E_\mu$) is used to calibrate the detector response. The details of energy resolution and efficiency of hadrons at ICAL can be found in Ref [23].

Muon energy bins (E_{μ^\pm} in GeV)	Range	Bin width
12	0.8-4.8	0.34
4	4.8-6.8	0.5
3	6.8-9.8	1
1	9.8-12.8	3
Hadron energy bins (E_{hadron} in GeV)		
2	0.0-2.0	1
2	2.0-8.0	3
1	8.0-13	5
Muon angle bins ($\cos \theta_{\mu^\pm}$)		
20	-1 - +1	0.1

Table 1: Optimized 3D binning scheme used for analyses.

3.1 The χ^2 Function

The oscillation parameters of the atmospheric neutrinos have been extracted with a χ^2 analysis. The re-weighted events, with detector resolutions and efficiencies folded in, are binned into the observed muon energy, muon direction and hadron energy. An optimized bin width have been used for these observables to get statistically significant event rates. The data has been divided into a total of 20 muon energy bins and 5 hadron energy bins with varying bin widths. A total of 20 muon direction bins for $\cos \theta_\mu$ in the range of -1 to 1, with equal bin width has been chosen. The above mentioned binning scheme is applied for both ν_μ and $\bar{\nu}_\mu$ events. The details of the binning scheme is shown in Table 1.

A ‘‘pulled’’ χ^2 [27] method based on Poisson probability distribution is used to compare the expected and observed data with inclusion of systematic errors. Five systematic errors used in analysis are: a 20% error on atmospheric neutrino flux normalization, 10% error on neutrino cross-section, an overall 5% statistical error, a 5% uncertainty due to zenith angle dependence of the fluxes, and an energy dependent tilt error, as considered in earlier ICAL analyses [12, 13].

In the method of pulls, systematic uncertainties and the theoretical errors are parameterized in terms of a set of variables ζ , called pulls. Due to the fine binning, some bins may have very small number of entries. Therefore, we use the poissonian definition of χ^2 given as

$$\chi^2(\nu_\mu) = \min \sum_{i,j,k} \left(2(N_{ijk}^{th'}(\nu_\mu) - N_{ijk}^{ex}(\nu_\mu)) + 2N_{ijk}^{ex}(\nu_\mu) \left(\ln \frac{N_{ijk}^{ex}(\nu_\mu)}{N_{ijk}^{th'}(\nu_\mu)} \right) \right) + \sum_n \zeta_n^2, \quad (3)$$

where

$$N_{ijk}^{th'}(\nu_\mu) = N_{ijk}^{th}(\nu_\mu) \left(1 + \sum_n \pi_{ijk}^n \zeta_n \right). \quad (4)$$

Here, N_{ijk}^{ex} are the observed number of reconstructed events, generated using true values of the oscillation parameters in i^{th} muon energy bin, j^{th} muon direction bin and k^{th} hadron energy bin. In Eq.(4), N_{ijk}^{th} are the number of theoretically predicted events generated by varying oscillation parameters, $N_{ijk}^{th'}$ show modified events spectrum due to different systematic uncertainties, π_{ijk}^n are the systematic shift in the events of the respective bins due to n^{th} systematic error. The variable ζ_n , the univariate pull variable, corresponds to the π_{ijk}^n uncertainty. An expression similar to Eq.(3) can be obtained for $\chi^2(\bar{\nu}_\mu)$ using reconstructed μ^+ event samples.

The functions $\chi^2(\nu_\mu)$ and $\chi^2(\bar{\nu}_\mu)$ are calculated separately for the independent measurement of neutrino and anti-neutrino oscillation parameters. The two χ^2 can be added to get the combined $\chi^2(\nu_\mu + \bar{\nu}_\mu)$ as

$$\chi^2(\nu_\mu + \bar{\nu}_\mu) = \chi^2(\nu_\mu) + \chi^2(\bar{\nu}_\mu). \quad (5)$$

3.2 Same True oscillation parameters for neutrinos and antineutrinos

In the present work, we investigate the scenario where the neutrino and antineutrino oscillations are different. However, we begin with the case where neutrinos and antineutrinos have identical oscillation parameters ($|\Delta m_{32}^2| = |\Delta \bar{m}_{32}^2|$, $\sin^2 \theta_{23} = \sin^2 \bar{\theta}_{23}$). The central true values of the oscillation parameters and their marginalization range used in the analysis are shown in Table 2. The χ^2 have been calculated as the function of the atmospheric oscillation parameters ($|\Delta m_{32}^2|$ and $\sin^2 \theta_{23}$) while all other oscillation parameters are kept fixed at their central values. The solar oscillation parameters Δm_{21}^2 and $\sin^2 \theta_{12}$ are fixed as they do not show significant impact on the results. Since θ_{13} is now known quite precisely, it has been kept fixed as well. Since, ICAL is not sensitive to the δ_{CP} [28], it is kept fixed at 0° .

In order to obtain the experimental sensitivity for $\sin^2 \theta_{23}$ and $|\Delta m_{32}^2|$, we independently minimize the $\chi^2(\nu_\mu)$, $\chi^2(\bar{\nu}_\mu)$ and combined $\chi^2(\nu_\mu + \bar{\nu}_\mu)$ function by varying oscillation parameters within their allowed ranges with all systematic uncertainties folded in. The precision on the oscillation parameters can

Oscillation parameters	True values	Marginalization range
$\sin^2(2\theta_{12})$	0.86	Fixed
$\sin^2(\theta_{23})$	0.5	0.4-0.6
$\sin^2(\theta_{13})$	0.0234	Fixed
Δm_{21}^2 (eV ²)	7.6×10^{-5}	Fixed
$ \Delta m_{32}^2 $ (eV ²)	2.4×10^{-3}	$(2.1-2.6) \times 10^{-3}$
δ	0.0	Fixed

Table 2: True values of the neutrino oscillation parameters used in the analysis. We vary $\sin^2 \theta_{23}$ and $|\Delta m_{32}^2|$ in their 3σ range whereas the other variables are kept fixed.

be defined as the ratio of $(P_{max} - P_{min})$ to the $(P_{max} + P_{min})$, where P_{max} and P_{min} are the maximum and minimum values of the concerned oscillation parameters at the given confidence level.

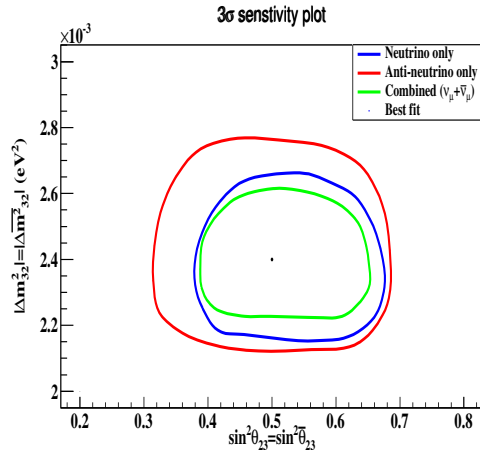


Figure 1: The 3σ sensitivity plot on $(\sin^2 \theta_{23} = \sin^2 \bar{\theta}_{23}, |\Delta m_{32}^2| = |\Delta \bar{m}_{32}^2|)$ parameter space from the χ^2 analyses separately for neutrino only events, anti-neutrino only events and combined neutrino and antineutrino ($\nu_\mu + \bar{\nu}_\mu$) events

Fig.1 shows the resulting contours at 3σ confidence level (C.L.) obtained for the $(|\Delta m_{32}^2|, \sin^2 \theta_{23})$ or $(|\Delta \bar{m}_{32}^2|, \sin^2 \bar{\theta}_{23})$ planes. These results are also compared with combined results of neutrino and antineutrino events.

Table 3 shows the precision values at the 3σ C.L. obtained from neutrino only events, anti-neutrino only events and with the combined ($\nu_\mu + \bar{\nu}_\mu$) events. It can be observed that combined ν_μ and $\bar{\nu}_\mu$ analysis gives more precise values of the oscillation parameters, as expected. The major contribution to this precision comes from the higher statistics of the combined neutrino events. However, the ICAL detector can also measure $|\Delta m_{32}^2|$ very precisely from neu-

Analysis	$\sin^2 \theta_{23}$	$ \Delta m_{32}^2 $ (eV ²)
Neutrino events	27.1%	10.4%
Anti-neutrino events	38.0%	13.4%
Combined($\nu_\mu + \bar{\nu}_\mu$)	25.0%	8.3%

Table 3: Precision values at the 3σ C.L. considering $\sin^2 \theta_{23} = \sin^2 \bar{\theta}_{23}$ and $|\Delta m_{32}^2| = |\Delta \bar{m}_{32}^2|$ (eV²) obtained from neutrino only events, anti-neutrino only events and with the combined ($\nu_\mu + \bar{\nu}_\mu$) events.

trino and antineutrino events, separately. It can be noted that the allowed parameter space of anti-neutrino analysis is wider than the neutrino only events analysis due to their low statistics.

3.3 Different True values of $|\Delta m_{32}^2|$ and $|\Delta \bar{m}_{32}^2|$

The good precision of INO-ICAL for $|\Delta m_{32}^2|$ and $|\Delta \bar{m}_{32}^2|$ motivates us to examine the scenario when the true values of $|\Delta m_{32}^2|$ and $|\Delta \bar{m}_{32}^2|$ have different values. This will allow us to either establish or rule out the hypothesis that neutrinos and antineutrinos have same oscillation parameters.

We assume that neutrinos and antineutrinos have different true values of mass squared differences ($|\Delta m_{32}^2|, |\Delta \bar{m}_{32}^2|$). All other oscillation parameters are same as in the previous section. We take different representative cases of the true values of $|\Delta m_{32}^2|$ and $|\Delta \bar{m}_{32}^2|$ and estimate χ^2 as a function of the $|\Delta m_{32}^2|$ and $|\Delta \bar{m}_{32}^2|$. For each case, the true values of all oscillation parameters are fixed and $\chi^2(\nu + \bar{\nu})$ have been estimated as a function of observed values of $|\Delta m_{32}^2|$ and $|\Delta \bar{m}_{32}^2|$. The χ^2 contours at 68%, 90% and 99% C.L. have been plotted on the ($|\Delta m_{32}^2|, |\Delta \bar{m}_{32}^2|$) parameter space. The straight line corresponding to the null hypothesis ($|\Delta \bar{m}_{32}^2| = |\Delta m_{32}^2|$) is also shown. If the null hypothesis line is $n\sigma$ away from the χ^2 minimum, it can be concluded that the null hypothesis ($|\Delta \bar{m}_{32}^2| = |\Delta m_{32}^2|$) is ruled out at $n\sigma$ C.L. The four plots in Fig. 2 correspond to the true values of $|\Delta m_{32}^2|$ and $|\Delta \bar{m}_{32}^2|$ as shown in Table 4.

Fig.2(a) show the contours when true values of $|\Delta m_{32}^2|$ and $|\Delta \bar{m}_{32}^2|$ are exactly equal (i.e. $|\Delta m_{32}^2| - |\Delta \bar{m}_{32}^2| = 0$). In this case, the null hypothesis line (solid black line) crosses the central best fit point. In Fig. 2(b), 2(c) and 2(d) the difference (i.e. $|\Delta m_{32}^2| - |\Delta \bar{m}_{32}^2|$) is non-zero, and hence the best fit point shifts away from the null hypothesis line. Fig.2(b) correspond to the case when true values of $|\Delta m_{32}^2| = 2.6 \times 10^{-3} eV^2$ and $|\Delta \bar{m}_{32}^2| = 2.2 \times 10^{-3} eV^2$ (i.e. $|\Delta m_{32}^2| - |\Delta \bar{m}_{32}^2| = 0.4 \times 10^{-3} eV^2$). Here, the null hypothesis line is tangential to 3σ contour. So, the tangential point is 3σ away from the central best fit value. Thus, it can be concluded that null hypothesis is ruled out at 3σ C.L. Similarly,

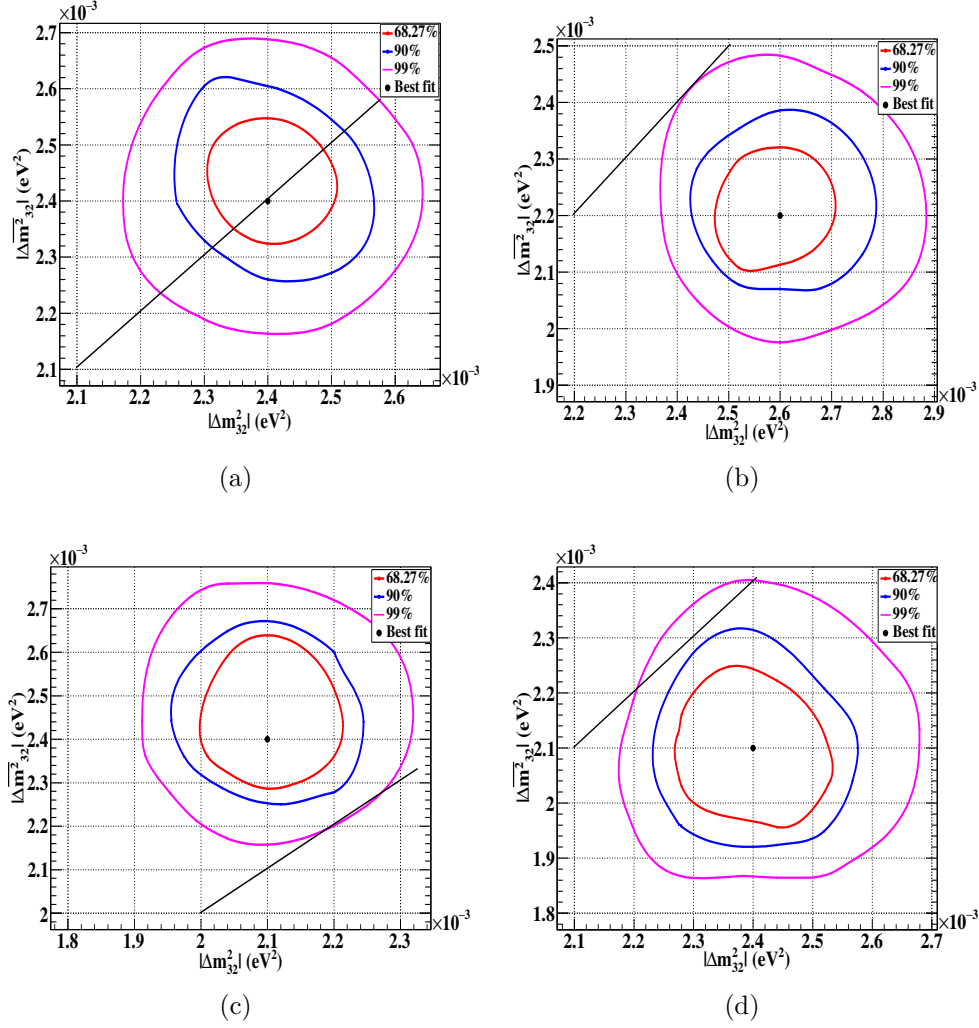


Figure 2: Contour plots at 68%, 90% and 99% C.L. for different true values of $|\Delta m_{32}^2|$ and $|\Delta \overline{m}_{32}^2|$ as mentioned in Table 4. Here, X-axis corresponds to $|\Delta m_{32}^2|$ values and Y-axis corresponds to $|\Delta \overline{m}_{32}^2|$ values.

Fig2.No.	$ \Delta m_{32}^2 (\text{eV}^2)$	$ \Delta \overline{m}_{32}^2 (\text{eV}^2)$	$ \Delta m_{32}^2 - \Delta \overline{m}_{32}^2 (\text{eV}^2)$
(a)	2.4×10^{-3}	2.4×10^{-3}	0.0×10^{-3}
(b)	2.6×10^{-3}	2.2×10^{-3}	0.4×10^{-3}
(c)	2.1×10^{-3}	2.4×10^{-3}	-0.3×10^{-3}
(d)	2.4×10^{-3}	2.1×10^{-3}	$+0.3 \times 10^{-3}$

Table 4: Different combinations of $|\Delta m_{32}^2|$ and $|\Delta \overline{m}_{32}^2|$ values used in Fig 2.

Fig. 2(c) shows that null hypothesis is tangential to 3σ CL when true values of $|\Delta m_{32}^2| = 2.1 \times 10^{-3} eV^2$ and $|\Delta \overline{m}_{32}^2| = 2.4 \times 10^{-3} eV^2$ (i.e. $|\Delta m_{32}^2| - |\Delta \overline{m}_{32}^2| = -0.3 \times 10^{-3} eV^2$). Fig.2(d) shows that the null hypothesis is ruled out at roughly 2.5σ CL when true value of $|\Delta m_{32}^2| = 2.4 \times 10^{-3} eV^2$ and $|\Delta \overline{m}_{32}^2| = 2.1 \times 10^{-3} eV^2$ (i.e. $|\Delta m_{32}^2| - |\Delta \overline{m}_{32}^2| = +0.3 \times 10^{-3} eV^2$).

3.4 ICAL sensitivity for $|\Delta m_{32}^2| - |\Delta \overline{m}_{32}^2| \neq 0$

In order to check the ICAL sensitivity for a non-zero value of the difference between $|\Delta m_{32}^2|$ and $|\Delta \overline{m}_{32}^2|$, the true values of $|\Delta m_{32}^2|$ and $|\Delta \overline{m}_{32}^2|$ have been varied independently in a range $(0.0021 - 0.0028 eV^2)$. But, we estimate the $\chi^2(\nu + \bar{\nu})$ only when the observed values of $|\Delta m_{32}^2|$ and $|\Delta \overline{m}_{32}^2|$ are equal. In other words, the $\chi^2(\nu + \bar{\nu})$ is being estimated on the null hypothesis line where the $|\Delta m_{32}^2|$ and $|\Delta \overline{m}_{32}^2|$ values are equal. The minimum value of χ^2 is chosen on this line that corresponds to the tangential point where the null hypothesis line coincides with the corresponding contour. Finally, this minimum χ^2 is binned as a function of difference in the true values of $(|\Delta m_{32}^2| - |\Delta \overline{m}_{32}^2|)$. This will result in several χ^2 points corresponding to a common $(|\Delta m_{32}^2| - |\Delta \overline{m}_{32}^2|)$ difference, depicted as dots in Fig.3. From all such candidate points, we pick those points that have the smallest χ^2 values and depict them as stars [see Fig.3].

For each value of $(|\Delta m_{32}^2| - |\Delta \overline{m}_{32}^2|)$, we calculate $\Delta\chi^2 = \chi^2 - \chi_{min}^2$ assuming $\chi_{min}^2 = 37$ and plot it as the functions of $|\Delta m_{32}^2| - |\Delta \overline{m}_{32}^2|$ in Fig 4. This figure depicts the INO-ICAL potential for ruling out the null hypothesis $|\Delta m_{32}^2| = |\Delta \overline{m}_{32}^2|$ and is our final result of the present study.

4 Results and Conclusions

The experimental confirmation of different sets of oscillation parameters for neutrinos and antineutrinos will be a signature of any new physics like CPT symmetry in the neutrino sector. In this paper, we investigate this possibility by studying INO-ICAL potential for the separate measurements of neutrino and antineutrino oscillation parameters for 10 years of exposure. The CC ν_μ and $\bar{\nu}_\mu$ events are separated into muon energy, muon direction and hadron energy bins. A χ^2 analysis is used with realistic detector resolutions, efficiencies and systematic errors. The separate analysis for neutrino and antineutrino events having identical oscillation parameters ($|\Delta m_{32}^2| = |\Delta \overline{m}_{32}^2|, \sin^2 \theta_{23} = \sin^2 \bar{\theta}_{23}$) indicates that ICAL can measure the atmospheric neutrino parameters $|\Delta m_{32}^2|$ with a precision of 10.14% and $\sin^2 \theta_{23}$ with a precision of 27.10%. The atmospheric antineutrino parameters $|\Delta \overline{m}_{32}^2|$ and $\sin^2 \bar{\theta}_{23}$ can be measured with a precision of 13.4% and 38.0% at 3σ confidence level respectively. As expected, the combined $\nu_\mu + \bar{\nu}_\mu$ events show a better sensitivity with a precision

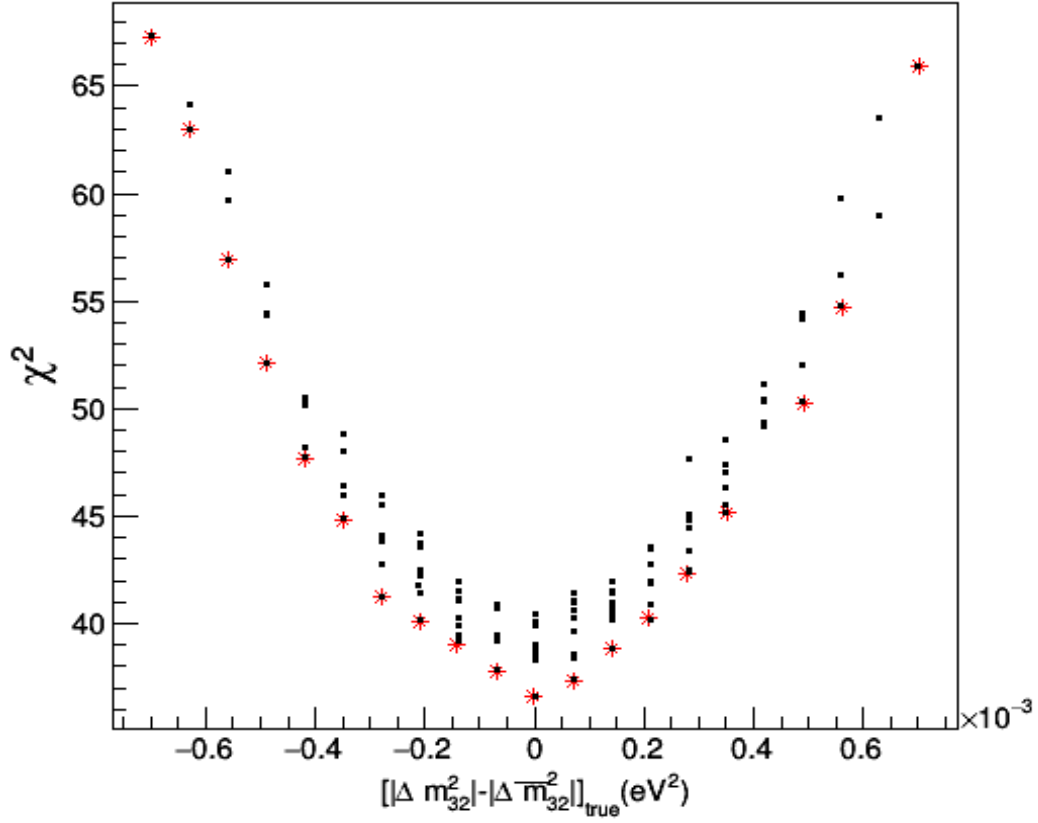


Figure 3: χ^2 versus $(|\Delta m_{32}^2| - |\Delta \overline{m}_{32}^2|)_{\text{true}} (eV^2)$ plot, black dots represents the several minimum χ^2 for a common $(|\Delta m_{32}^2| - |\Delta \overline{m}_{32}^2|)$ difference and red stars depicts the smallest χ^2 value among all of them.

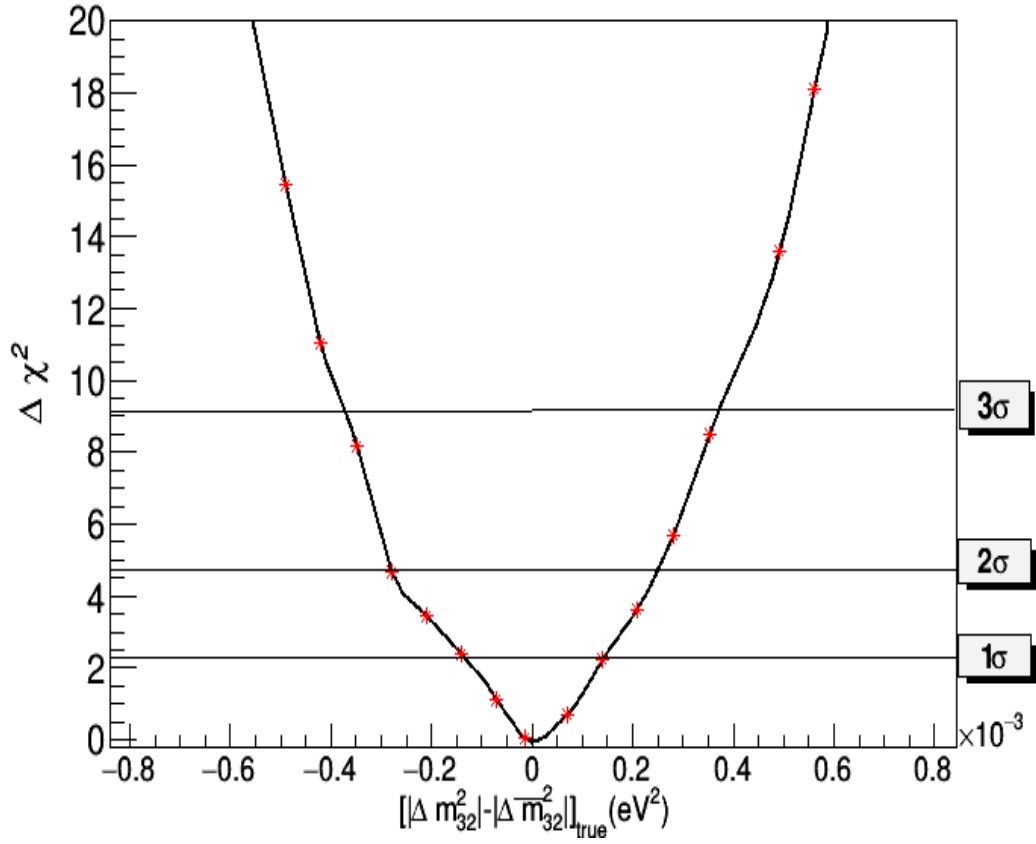


Figure 4: The INO-ICAL sensitivity for $(|\Delta m_{32}^2| - |\Delta \overline{m}_{32}^2|)_{True}(eV^2)$ at 1σ , 2σ and 3σ confidence levels.

of 8.7% for $|\Delta m_{32}^2|$ and 25.0% for $\sin^2 \theta_{23}$ at same confidence level due to larger events in χ^2 .

Further, we investigate the scenario where the neutrino and antineutrino oscillation parameters have different values. We measure the ICAL sensitivity for ruling out the null hypothesis ($|\Delta m_{32}^2| = |\overline{\Delta m}_{32}^2|$) by estimating the difference between the true values of mass squared differences of neutrinos and antineutrinos i.e. ($|\Delta m_{32}^2| - |\overline{\Delta m}_{32}^2|$). We show that ICAL can rule out the null hypothesis of $|\Delta m_{32}^2| = |\overline{\Delta m}_{32}^2|$ at more than 3σ level if the difference of true values of $|\Delta m_{32}^2| - |\overline{\Delta m}_{32}^2| \geq +0.4 \times 10^{-3} eV^2$ or $|\Delta m_{32}^2| - |\overline{\Delta m}_{32}^2| \leq -0.4 \times 10^{-3} eV^2$.

5 Acknowledgment

The authors would like to thank Department of Science and Technology (DST), Govt. of India for their generous funding support. We would also like to thank University of Delhi for providing R & D grants to carry out a part of this work.

References

- [1] Super-Kamiokande Collaboration, Y.Fukuda et al., “*Evidence for Oscillation of Atmospheric Neutrinos*”, Phys. Rev. Lett. **81**, 1562(1998).
- [2] Super-Kamiokande Collaboration, Y.Fukuda et al., “*Measurement of the Flux and Zenith-Angle Distribution of Upward Throughgoing Muons by Super-Kamiokande*”, Phys. Rev. Lett. **82**, 2644 (1999).
- [3] SNO, Q. R. Ahmad et al., “*Direct Evidence for Neutrino Flavor Transformation from Neutral-Current Interactions in the Sudbury Neutrino Observatory*”, Phys. Rev. Lett. **89**, 011301 (2002).
- [4] KamLAND, K. Eguchi et al., “*First results from KamLAND: Evidence for reactor anti- neutrino disappearance*”, Phys. Rev. Lett. **90**, 021802 (2003).
- [5] B. Pontecorvo, “*mesonium and anti-mesonium*”, Zh. Eksp. Theor. Fiz. **33**, 549 (1957).
- [6] B. Pontecorvo, Sov. Phys. JETP **26**, 984 (1968) [Zh. Eksp. Teor. Fiz 53, 1717 (1967)].
- [7] INO Collaboration, S.Atthar et al., *The Technical Design Report of INO-ICAL Detector* (2006).
- [8] The ICAL Collaboration, “*Physics Potential of the ICAL detector at the India-based Neutrino Observatory (INO)*”, arXiv:1505.07380v1 [physics.ins-det](2015).

- [9] M. M. Medeiros et al. "Neutrino and Antineutrino Oscillation Parameters Measured by the MINOS Atmospheric and Beam Data", Proceedings, 33rd International Cosmic Ray Conference (ICRC2013), Braz.J.Phys. **44**, no.5, pp.415-608 (2014).
- [10] K. Abe et al. (Super-Kamiokande Collaboration), "Search for Differences in Oscillation Parameters for Atmospheric Neutrinos and Antineutrinos at Super-Kamiokande", Phys. Rev. Lett. **107**, 241801 (2011).
- [11] A. Ghosh et al., "Determining the neutrino mass hierarchy with INO, T2K, NOvA and reactor experiments", JHEP **04**, 009 (2013).
- [12] T. Thakore et al., The reach of INO for atmospheric neutrino oscillation parameters, JHEP **05**, 058 (2013).
- [13] D. Kaur et al., "INO-ICAL detector sensitivity for the neutrino oscillation parameters", Euro. Phys. J. C, **75:156** (2015).
- [14] M. M. Devi et al., "Enhancing sensitivity to neutrino parameters at INO combining muon and hadron information", JHEP **10**, 189 (2014).
- [15] Animesh Chatterjee, Raj Gandhi, Jyotsna Singh, "Probing Lorentz and CPT Violation in a Magnetized Iron Detector using Atmospheric Neutrinos", JHEP **06**, 045 (2014), arXiv:1402.6265v1 [hep-ph].
- [16] A. Dutta et al., "Atmospheric neutrinos as a probe of CPT violation", Phys. Letter B, 597, 356361 (2004).
- [17] M. C. Gonzalez-Garcia, M. Maltoni, and T. Schwetz, "Status of the CPT violating interpretations of the LSND signal", Phys. Rev. D **68**, 053007 (2003).
- [18] G. Barenboim and J. Lykken, "MINOS and CPT-violating neutrinos", Phys. Rev. D **80**, 113008 (2009).
- [19] D. Kaur et al., "Characterisation of 3 mm glass electrodes and development of RPC detector for INO-ICAL experiment", Nuclear Instrumentation and Methods (NIM) **A 774** (2015).
- [20] A. Ghosh, S. Choubey, "Measuring the Mass Hierarchy with Muon and Hadron Events in Atmospheric Neutrino Experiments", JHEP 2013,174 (2013).
- [21] GEANT simulation toolkit wwwasd.web.cern.ch/wwwasd/geant/

- [22] A. Chatterjee et al., “*A Simulations Study of the Muon Response of the Iron Calorimeter Detector at the India-based Neutrino Observatory*”, JINST **9** P007001 (2014).
- [23] M. M. Devi et al., “*Hadron energy response of the Iron Calorimeter detector at the India-based Neutrino Observatory*”, JINST **8** P11003 (2013).
- [24] M. Honda, T.Kajita et al, “*New calculation of the atmospheric neutrino flux in a three-dimensional scheme*”, Phys. Rev. D **70**, [arXiv:0404457][astro-ph] (2004).
- [25] D. Casper, “*The nuance Neutrino Simulation, and the Future*”, Nucl.Phys. Proc.Suppl. **112**, 161 [arXiv:0208030][hep-ph](2002).
- [26] A. M. Dziewonski and D. L. Anderson, “*Preliminary reference earth model*”, Phys. Earth Planet. Interior **25**, 297-356, (1981).
- [27] M. C. Gonzalez-Garcia, M. Maltoni et al, “*Atmospheric neutrino oscillations and new physics*”, Phys.Rev. D **70**, 033010 (2004), [arXiv:0404085v1][hep-ph].
- [28] A. Ghosh et al., “*Determining the neutrino mass hierarchy with INO, T2K, NO ν A and reactor experiments*”, JHEP **4**, 009(2013).